558226

ENTERED

Sandia National Laboratories
Waste Isolation Pilot Plant

Analysis Package for Direct Brine Releases: 2012 Panel Closure System Performance Assessment (PCS-2012 PA)

Author:	Bwalya Malama		09/28/12
	Print	Signature	Date
Technical Review:	Chris Camphouse		9/28/12
	Print	Signature	Date
QA Review:	Shelly R. Nielsen	Shelly R. Nielsen	10-1-12
	Print	Signature	Date
Management Review:	Sean Dunagan		9/28/12
	Print	Signature	Date

WIPP:1.4.1:PA:QA-L:557393

Information Only

120951

Table of Contents

1 Introduction 5
2 Background 6
3 Approach 8
3.1 Model Geometry 8
3.2 Initial Conditions 10
4 Calculation Methodology 11
4.1 Modeled Scenarios 11
4.1.1 Scenario 1 (S1-DBR) 11
4.1.2 Scenario 2 (S2-DBR) 12
4.1.3 Scenario 3 (S3-DBR) 12
4.1.4 Scenario 4 (S4-DBR) 13
4.1.5 Scenario 5 (S5-DBR) 13
4.2 Run Control 13
5 Results 14
5.1 Summary 14
5.2 Direct Brine Releases from the Lower Drilling Location 15
5.3 Sensitivity of Direct Brine Releases to Input Parameters 27
6 Conclusions 31
7 References 31

Information Only

List of Tables

Table 4-1: Scenarios used in BRAGFLO Salado flow modeling. 11
Table 4-2: Intrusion times modeled by DBR for each scenario. 12
Table 5-1: Summary statistics for the PCS-2012 PA and PABC-2009 DBR calculations over all replicates and vectors. 15
Table 5-2: Summary table of number of vectors with non-zero, maximum and average DBR volumes over all three replicates for the S1-DBR calculations 17
Table 5-3: Summary table of number of vectors with non-zero, maximum and average DBR volumes over all three replicates for the S2-DBR calculations. 18
Table 5-4: Summary table of number of vectors with non-zero, maximum and average DBR volumes over all three replicates for the S3-DBR calculations. 19
Table 5-5: Summary table of number of vectors with non-zero, maximum and average DBR volumes over all three replicates for the S4-DBR calculations. 20
Table 5-6: Summary table of number of vectors with non-zero, maximum and average DBR volumes over all three replicates for the S5-DBR calculations. 21

List of Figures

Figure 3-1: PCS-2012 PA DBR material map (logical grid) with ROM salt PCS. 8
Figure 3-2: PABC-2009 DBR material map (logical grid) with Option D panel closure (after Clayton et al., 2010). 9
Figure 3-3. Regions to be used to transfer initial pressure and saturation between the 10,000 year BRAGFLO grid and the DBR grid for the PABC-2009. 10
Figure 5-1: PCS-2012 PA lower intrusion DBR volume percentile rankings for all replicates and vectors of the scenario S1-DBR. 22
Figure 5-2: PABC-2009 lower intrusion DBR volume percentile rankings for all replicates and vectors of scenario S1-DBR. 22
Figure 5-3: PCS-2012 PA lower intrusion DBR volume percentile rankings for all replicates and vectors of scenario S2-DBR. 23
Figure 5-4: PABC-2009 lower intrusion DBR volume percentile rankings for all replicates and vectors of scenario S2-DBR. 23
Figure 5-5: PCS-2012 PA lower intrusion DBR volume percentile rankings for all replicates and vectors of scenario S3-DBR. 24
Figure 5-6: PABC-2009 lower intrusion DBR volume percentile rankings for all replicates and vectors of scenario S3-DBR. 24
Figure 5-7: PCS-2012 PA lower intrusion DBR volume percentile rankings for all replicates and vectors of scenario S4-DBR. 25
Figure 5-8: PABC-2009 lower intrusion DBR volume percentile rankings for all replicates and vectors of scenario S4-DBR. 25
Figure 5-9: PCS-2012 PA lower intrusion DBR volume percentile rankings for all replicates and vectors of scenario S5-DBR. 26
Figure 5-10: PABC-2009 lower intrusion DBR volume percentile rankings for all replicates and vectors of scenario S5-DBR. 26

Information Only

Figure 5-11: Scatter plot of DBR volume versus pressure in the intruded panel for replicate 1, S2-DBR scenario, lower drilling intrusion, PCS-2012 PA. Symbols indicate intrusion times in years. 28
Figure 5-12: Scatter plot of DBR volume versus pressure in the intruded panel for replicate 1, S2-DBR scenario, lower drilling intrusion, PABC-2009. Symbols indicate intrusion times in years. 28
Figure 5-13: Scatter plot of DBR volume versus pressure in the intruded panel for replicate 1, S2-DBR scenario, lower drilling intrusion, PCS-2012 PA. Symbols indicate the range of mobile brine saturation (dimensionless). 29
Figure 5-14: Scatter plot of DBR volume versus pressure in the intruded panel for replicate 1, S2-DBR scenario, lower drilling intrusion, PABC-2009. Symbols indicate the range of mobile brine saturation (dimensionless). 29
Figure 5-15: Scatter plot of mobile brine saturation versus pressure for replicate 1, S2-DBR scenario, lower drilling intrusion, all intrusion times, PCS-2012 PA. Symbols indicate the range of DBR volumes in m^3. 30
Figure 5-16: Scatter plot of mobile brine saturation versus pressure for replicate 1, S2-DBR scenario, lower drilling intrusion, all intrusion times, PABC-2009. Symbols indicate the range of DBR volumes in m^3. 30

Information Only

1 INTRODUCTION

The Waste Isolation Pilot Plant (WIPP), located in southeastern New Mexico, has been developed by the U.S. Department of Energy (DOE) for geologic (deep underground) disposal of transuranic (TRU) waste. Containment of TRU waste at the WIPP is regulated by the U.S. Environmental Protection Agency (EPA) according to the regulations set forth in Title 40 of the Code of Federal Regulations (CFR), Part 191. The DOE demonstrates compliance with the containment requirements according to the Certification Criteria in Title 40 CFR Part 194 by means of performance assessment (PA) calculations performed by Sandia National Laboratories (SNL). WIPP PA calculations estimate the probability and consequence of potential radionuclide releases from the repository to the accessible environment for a regulatory period of 10,000 years after facility closure. The models used in PA are maintained and updated with new information as part of an ongoing process. Improved information regarding important WIPP features, events, and processes typically results in refinements and modifications to PA models and the parameters used in them. Planned changes to the repository and/or the components therein also result in updates to WIPP PA models. WIPP PA models are used to support the repository recertification process that occurs at five-year intervals following the receipt of the first waste shipment at the site in 1999.

Waste panel closures comprise a repository feature that has been represented in WIPP PA since the original Compliance Certification Application (CCA) of 1996. Panel closures are included in WIPP PA models principally because they are a part of the disposal system, not because they play a substantive role in inhibiting the release of radionuclides to the outside environment. The DOE stated in the CCA (DOE 1996) that *"The panel closure system was not designed or intended to support long-term repository performance."* The 1998 rulemaking that certified WIPP to receive transuranic waste placed conditions on the panel closure design to be implemented in the repository. The mandated design consists of a concrete block wall, an open drift section, and a concrete monolith, and was termed the "Option D" panel closure. Following the selection of the Option D design in 1998, the engineering of the panel closure has been re-assessed, and a revised design has been established that is simpler, cheaper, and easier to construct. The revised panel closure design, termed the Run-of-Mine Panel Closure System (ROMPCS), is comprised of 100 feet of ROM salt with barriers at each end. The ROM salt is generated from ongoing mining operations at the WIPP and may be compacted and/or moistened as it is emplaced in a panel entry. The barriers consist of ventilation bulkheads, similar to those currently used in the panels as room closures.

The DOE has submitted a planned change request (PCR) to the EPA requesting that the EPA modify Condition 1 of the Final Certification Rulemaking for 40 CFR Part 194 (EPA, 1998) for the WIPP. The PCR submitted to EPA requests that Condition 1 be changed, and that the ROMPCS design be approved for use in all panels (DOE, 2011). In support of this rulemaking change, a performance assessment has been completed that incorporates the ROMPCS design into the current PA baseline established by the 2009 Performance Assessment Baseline Calculation, referred to hereafter as PABC-2009 (Clayton et al., 2010). The name given to this new panel closure PA is PCS-2012, and the plan for its execution is detailed in AP-161 (Camphouse 2012a). PCS-2012 PA results are compared to those obtained in the PABC-2009 as

Information Only

a means to quantify potential impacts due to the panel closure redesign. This analysis package details the analysis of direct brine releases (DBRs) of the PCS-2012 PA.

2 BACKGROUND

DBRs are releases of contaminated brine originating in the repository and flowing up an intrusion borehole during the period of drilling. In order for DBR to occur, two criteria must be satisfied (Stoelzel and O'Brien 1996):

1. Volume averaged brine pressure in the vicinity of the repository encountered by drilling must exceed drilling fluid hydrostatic pressure (calculated to be 8 MPa).
2. Brine saturation in the repository must exceed the residual brine saturation of the waste material (sampled from a uniform distribution ranging from 0.0 to 0.552).

If both of these criteria are met, a DBR is calculated using the multi-phase flow code BRAGFLO with a two dimensional, semi-horizontally oriented grid, which represents the vicinity of the waste panels. If either of these conditions is not satisfied, no DBR is calculated.

DBRs are calculated from the following well deliverability equation in BRAGFLO (Mattax and Dalton 1990):

$$q_p(t) = J_p\left(P_p(t) - P_{wf}\right) \tag{1}$$

where $q_p(t)$ is the volumetric brine flux to the well as a function of time, J_p is the well productivity index, $P_p(t)$ is the volume averaged brine pressure of the repository in the vicinity of the intrusion as a function of time, and P_{wf} is the flowing bottom-hole pressure (assumed to be constant during each drilling intrusion). The flowing bottom-hole pressure is defined as the dynamic pressure at the inlet to the wellbore adjacent to the point of entry into the repository. It is less than the static pressure due to elevation, friction and acceleration effects (Stoelzel and O'Brien 1996).

The well productivity index, J_p, quantifies how readily brine can enter the well and flow to the surface. It is calculated from the following equation (Mattax and Dalton 1990; Chappelear and Williamson 1981):

$$J_p = \frac{2\pi k k_{rp} h}{\mu_p\left[\ln\left(\frac{r_e}{r_w}\right) + s - \frac{1}{2}\right]} \tag{2}$$

where

k Intrinsic permeability of the waste (constant: 2.4 x 10^{-13} m^2, WAS_AREA:PRMX_LOG)

k_{rp} Relative permeability of the waste assuming the modified Brooks-Corey relative permeability model: $k_{rp} = S_{el}^{(2+3\lambda)/\lambda}$, where λ is the pore distribution parameter (WAS_AREA:PORE_DIS), S_{el} is the effective brine saturation without correction for

Information Only

residual gas saturation $S_{e1} = (S_b - S_{br})/(1 - S_{br})$, S_b is the brine saturation, and S_{br} is the residual brine saturation (WAS_AREA:SAT_RBRN)

h Crushed panel height, defined as $h = h_i(1-\phi_i)/(1-\phi)$, where h_i is initial panel height (3.96 m), ϕ_i is the initial room-scale porosity (0.848, WAS_AREA:POROSITY)), and ϕ is the room-scale porosity at the time of intrusion (calculated by BRAGFLO see Helton et al. 1998)

μ Brine dynamic viscosity (0.0021 Pa-s, BRINESAL:VISCO)

r_e Equivalent drainage radius of the grid block containing the well and is defined by $r_e = \sqrt{(\Delta x)(\Delta y)/\pi}$, where Δx and Δy are the grid cell dimensions of the grid cell containing the well.

r_w Well radius (0.1556 m, assuming a 12.25 in. drill bit diameter, BOREHOLE:DIAMMOD divided by two)

s Skin factor (enhanced well productivity due to the presence of a cavity at base of well)

The skin factor is calculated using (Lee 1982):

$$s = \left(\frac{k}{k_s} - 1\right)\ln\left(\frac{r_w}{r_s}\right), \tag{3}$$

where k_s is the permeability of an open channel as a result of cuttings, cavings and spallings releases, and r_s is the effective radius of the well bore with the cuttings, cavings and spallings volume (V_i) removed.

The effective radius r_s is obtained by converting the cuttings, cavings and spallings volume removed into a cylinder of equal volume with the initial height of the waste (h_i), and then computing the radius of the cylinder:

$$r_s = \sqrt{\frac{V_i}{h_i \pi}}. \tag{4}$$

For all WIPP PA calculations, k_s is assumed to be infinite, in which case Equation (3) simplifies to

$$s = \ln\left(\frac{r_w}{r_s}\right). \tag{5}$$

DBRs are calculated using the code BRAGFLO and a two-dimensional near-horizontal grid that dips 1° to the south. Five scenarios were simulated and are discussed in section 4.1.

Information Only

3 APPROACH

The conceptual models implemented in the PCS-2012 PA calculations are unchanged from those used in the PABC-2009 (Clayton et al., 2010). Changes incorporated in the PCS-2012 PA DBR calculations to model the ROMPCS are discussed below.

3.1 Model Geometry

The scenarios used for the PCS-2012 PA are the same as those used for the PABC-2009. The DBR numerical grid and material map used in the PCS-2012 PA calculations is shown in Figure 3-1. Note that the color scheme in Figure 3-1 has been chosen so as to correspond to the color scheme used in the PCS-2012 PA BRAGFLO grid and material map (Figure 3-4 to Figure 3-8 in Camphouse 2012b). The PABC-2009 DBR numerical grid and material map is shown in Figure 3-2.

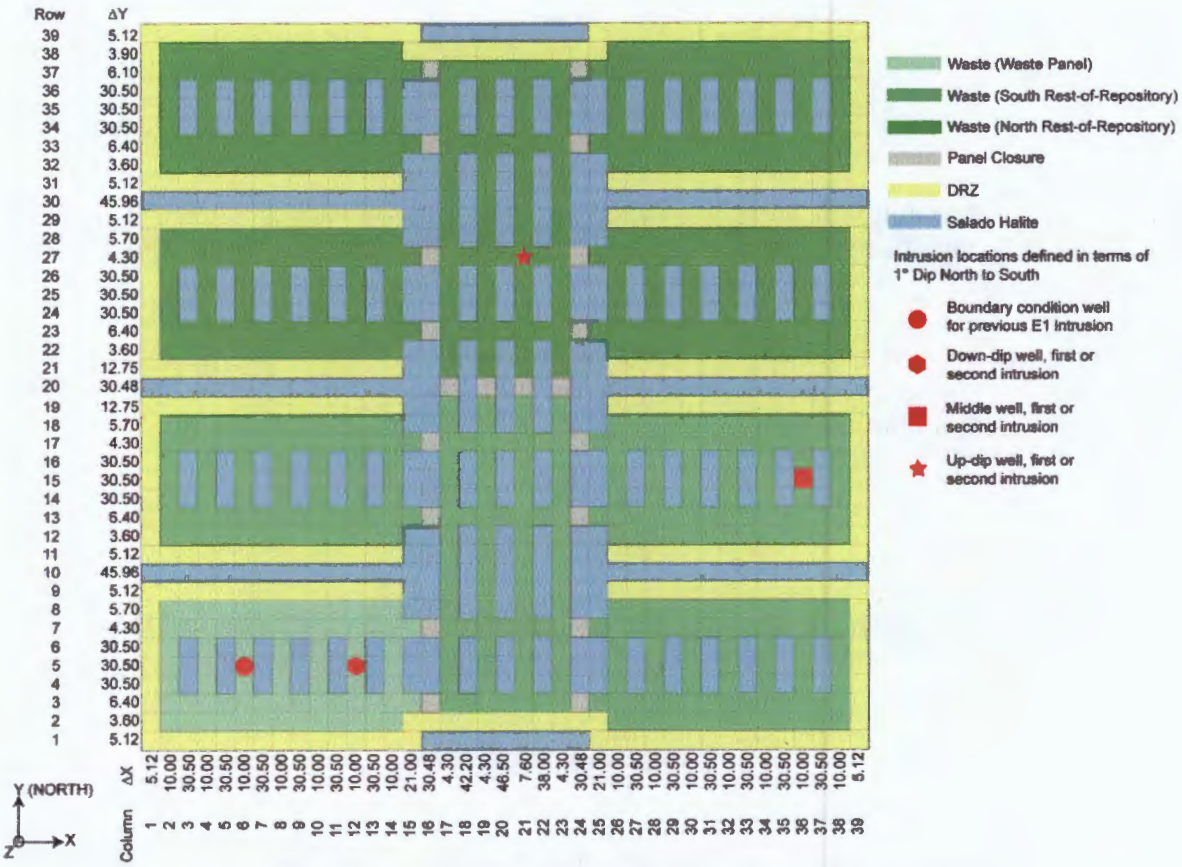

Figure 3-1: PCS-2012 PA DBR material map (logical grid) with ROM salt PCS.

The Option D panel closure modeled in the PABC-2009 is 40 meters long whereas the ROMPCS modeled in the PCS-2012 PA is 30.48 meters (100 feet) long. As a result, grid cell lengths corresponding to panel closures were reduced to 30.48 meters in the PCS-2012 PA. In addition,

Information Only

the ROMPCS, which is modeled as run-of-mine salt in the PCS-2012 PA, has no concrete component that is "keyed in" to the surrounding DRZ. As a result, material elements corresponding to equivalent DRZ/concrete in the PABC-2009 are replaced by DRZ in the PCS-2012 PA.

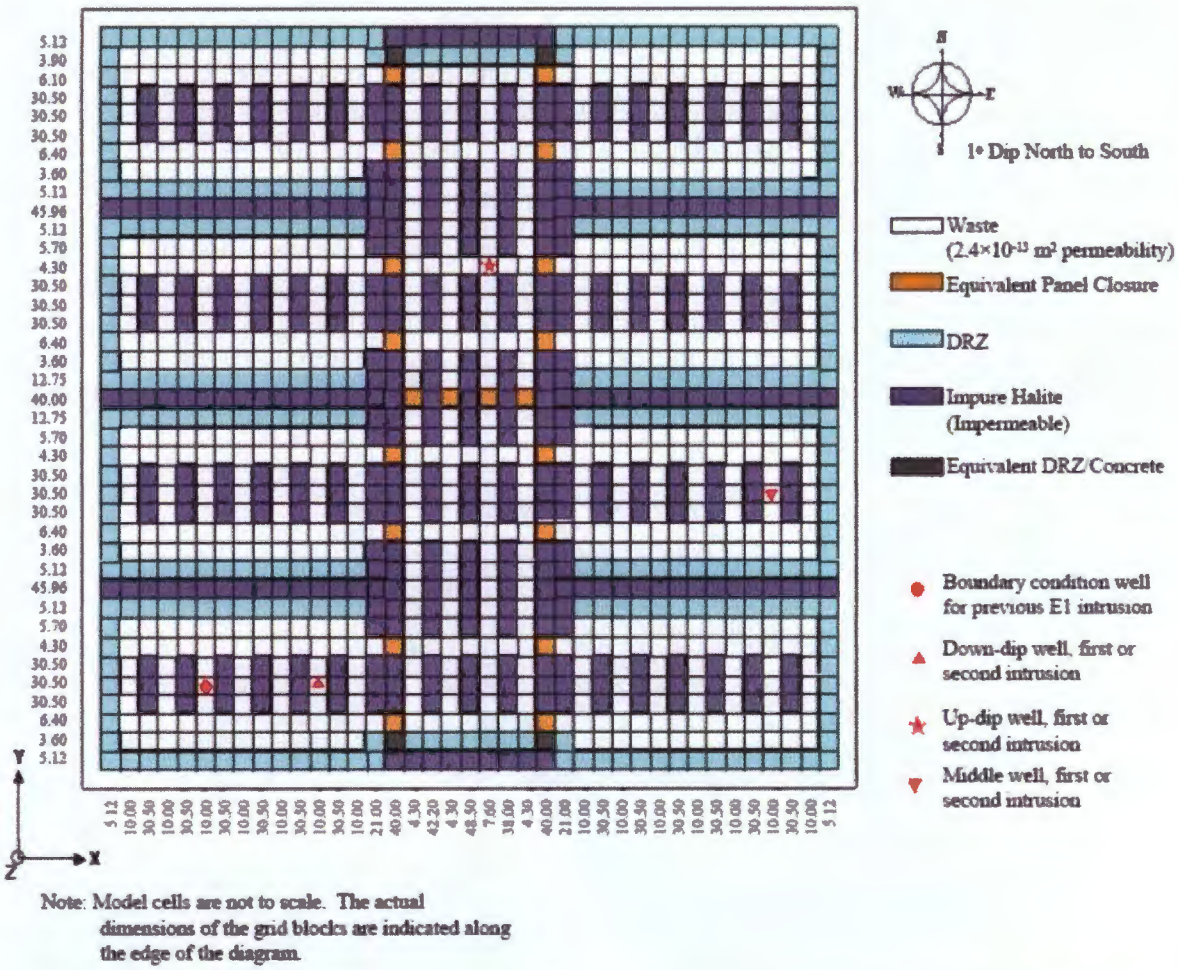

Figure 3-2: PABC-2009 DBR material map (logical grid) with Option D panel closure (after Clayton et al., 2010).

To calculate DBR volumes the same three drilling locations considered in PABC-2009 are considered in PCS-2012, namely: upper (up-dip), middle and lower (down-dip) locations. These are shown in Figure 3-1 (compare with Figure 3-2). Some of the calculations for DBR are for a drilling intrusion preceded by an earlier intrusion in either the same or different waste panel. The effects of these prior intrusions are incorporated into the calculations by specifying a boundary or initial condition well at their grid location, denoted by the red dot in Figure 3-1. The properties of the boundary condition well depend on the type of the prior intrusion and the time that has elapsed since its occurrence.

Information Only

3.2 Initial Conditions

Volume averaged brine pressures and brine saturations are calculated from the 10,000 year BRAGFLO simulations. The BRAGFLO results, corresponding to the time of intrusion, are used in the DBR simulations as initial conditions. The waste regions in the BRAGFLO grid and the DBR grid are each divided into three regions and volume-averaged brine pressure and saturations are transferred from corresponding regions in the BRAGFLO grid to the DBR grid. These regions corresponded to the single waste panel, south rest of repository (SRR), and north rest of repository (NRR). This method ensures that the relative volumes of these regions are equal between the 10,000 year BRAGFLO runs and the DBR runs. The definition of these repository regions can be seen in Figure 3-1.

Figure 3-3 illustrates the method used to transfer initial conditions in the waste for the PCS-2012 PA, which is unchanged from the PABC-2009 DBR runs. The volume averaged pressure and saturation from the three waste-filled regions in the BRAGFLO grid (WAS_AREA, SRR, NRR) at the time of the intrusion are used as the initial pressure and saturation for the three waste regions in the DBR grid (Lower, Middle, and Upper, respectively). The pressure and saturation can change during the DBR calculations.

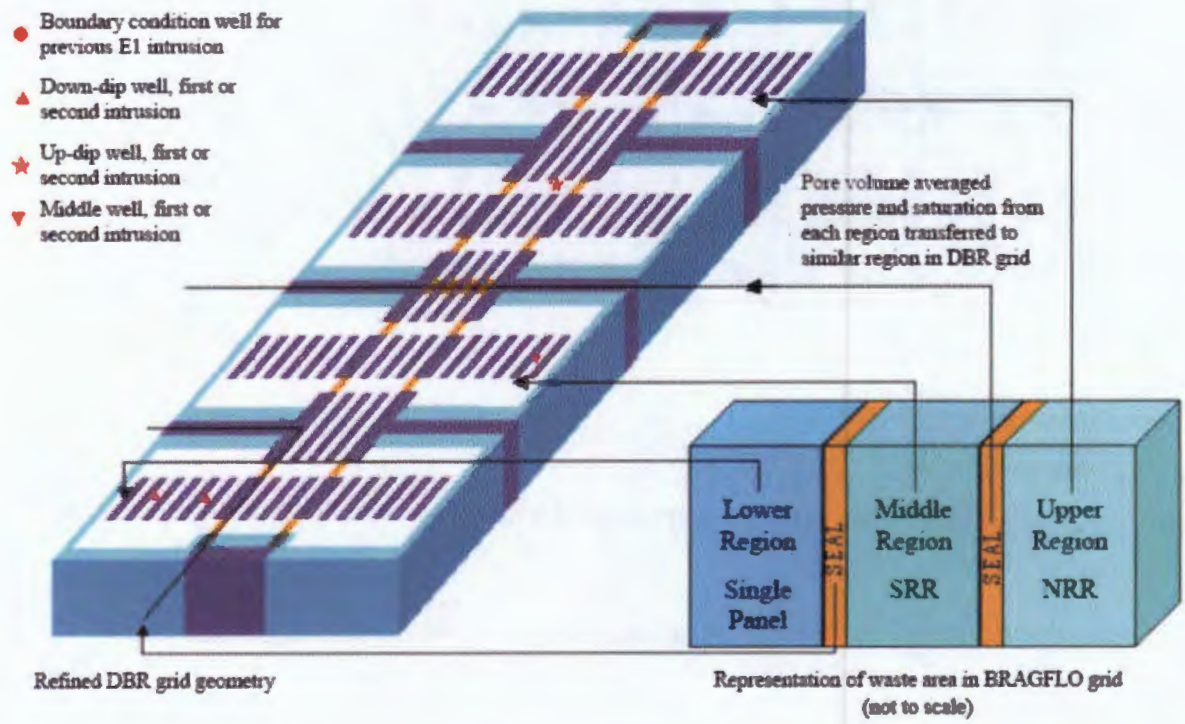

Figure 3-3. Regions to be used to transfer initial pressure and saturation between the 10,000 year BRAGFLO grid and the DBR grid for the PABC-2009.

Information Only

4 CALCULATION METHODOLOGY

DBR calculations are divided into five scenarios. Each DBR scenario represents an intrusion into the repository due to a drilling event. The initial conditions for the DBR simulations are obtained from the BRAGFLO Salado Flow simulations (Camphouse, 2012b) using an appropriate scenario and at an appropriate time for the particular drilling intrusion time. An E1 intrusion scenario is defined as an intrusion into the repository, which creates a pathway to a pressurized brine pocket below the repository. An E2 intrusion scenario is defined as an intrusion into the repository that terminates in the repository and does not create a pathway to a pressurized brine pocket below the repository. The results of the DBR calculations are the volumes of brine that leave the repository and reach the surface at the time of drilling and up to 4.5 days after. These results are used by the code CCDFGF to interpolate volumes of waste for the specific conditions that arise in a given future (location and timing of future drilling intrusions).

4.1 Modeled Scenarios

Below an overview is given of the DBR calculations performed for the PCS-2012 PA. In performing DBR calculations, the five BRAGLFO scenarios S1-BF to S5-BF used in Salado flow modeling are used to set volume-averaged brine pressure and brine saturation in the DBR calculations at the time of intrusion. These BRAGFLO Salado flow scenarios are listed in Table 4-1.

Table 4-1: Scenarios used in BRAGFLO Salado flow modeling.

Scenario	Description
S1-BF	Undisturbed Repository
S2-BF	E1 intrusion at 350 years
S3-BF	E1 intrusion at 1,000 years
S4-BF	E2 intrusion at 350 years
S5-BF	E2 intrusion at 1,000 years

With the brine pressure and brine saturation transferred from the Salado flow results, DBR calculations quantify impacts due to initial or subsequent intrusions into the repository. DBR simulations cover a range of intrusion scenarios, locations, and timing using five scenarios, S1-DBR to S5-DBR. A summary of intrusion times for each scenario is given in Table 4-2.

4.1.1 Scenario 1 (S1-DBR)

The BRAGFLO Salado modeling results from the S1-BF scenario are used as initial conditions to construct the first intrusion into the repository in which a DBR may occur. In the BRAGFLO Salado flow modeling (Camphouse, 2012b), this scenario represents an undisturbed repository. In the computation of DBRs for this scenario, upper, middle, and lower drilling intrusions are

Information Only

modeled at 100, 350, 1,000, 3,000, 5,000, and 10,000 years (3 locations × 6 intrusion times × 100 vectors = 1,800 calculations per replicate).

Table 4-2: Intrusion times modeled by DBR for each scenario.

Scenario	Intrusion times (years)
S1-DBR	100, 350, 1000, 3000, 5000, 10000
S2-DBR	550, 750, 2000, 4000, 10000
S3-DBR	1200, 1400, 3000, 5000, 10000
S4-DBR	550, 750, 2000, 4000, 10000
S5-DBR	1200, 1400, 3000, 5000, 10000

4.1.2 Scenario 2 (S2-DBR)

The BRAGFLO Salado flow modeling results from the S2-BF scenario are used as initial conditions to construct a second or subsequent intrusion into the repository in which a DBR may occur and in which the first intrusion had intersected a pressurized Castile brine reservoir at 350 years (Camphouse, 2012b). For the second or subsequent intrusion, upper, middle, and lower drilling intrusions were modeled at 550, 750, 2,000, 4,000 and 10,000 years (3 locations × 5 intrusion times × 100 vectors = 1,500 calculations per replicate). The effect of the prior E1 intrusion is incorporated in the calculations by the specification of a boundary condition well as denoted by the red dot in Figure 3-1. The properties of the boundary condition well correspond to the properties at the time of the second intrusion.

Runs for the lower drilling location assume that the second or subsequent intrusion occurs at the location labeled in Figure 3-1 as the "down-dip well". This represents an intrusion in the same panel that was intersected by a previous intrusion (assumed to be at the location labeled "boundary condition well") and therefore the abandoned borehole still connects the panel with the brine reservoir. Runs for the middle drilling location assume that the second or subsequent intrusion occurs at the location labeled in Figure 3-1 as the "middle well"; a previous intrusion is assumed to have occurred at the location labeled "boundary condition well," which is in an adjacent panel. Runs for the upper drilling location assume that the second or subsequent intrusion occurs at the location labeled "up-dip well" in Figure 3-1; a previous intrusion is assumed to have occurred at the location labeled "boundary condition well," which is in a panel that is not adjacent to the current intrusion.

4.1.3 Scenario 3 (S3-DBR)

The BRAGFLO Salado modeling results from the S3-BF scenario are used as initial conditions to construct a second or subsequent intrusion into the repository in which a DBR may occur and in which the first intrusion had intersected a pressurized Castile brine reservoir at 1,000 years (Camphouse, 2012b). Upper, middle, and lower second or subsequent intrusions are modeled at 1,200, 1,400, 3,000, 5,000 and 10,000 years (3 locations × 5 intrusion times × 100 vectors =

Information Only

1,500 calculations per replicate). The effect of the prior E1 intrusion and the lower, middle, and upper drilling locations are treated the same as for the S2-DBR scenario.

4.1.4 Scenario 4 (S4-DBR)

For this scenario, the BRAGFLO Salado flow modeling results from the S4-BF scenario are used as initial conditions to construct a second or subsequent intrusion into the repository in which a DBR may occur and in which the first intrusion occurs at 350 years without hitting a Castile brine reservoir (Camphouse, 2012b). Upper, middle, and lower second or subsequent intrusions are modeled at 550, 750, 2,000, 4,000 and 10,000 years (3 locations × 5 intrusion times × 100 vectors = 1,500 calculations per replicate). Runs for the lower drilling location assume the second or subsequent intrusion occurs at the location labeled in Figure 3-1 as the "down-dip well". This represents an intrusion into the same panel that was intersected by a previous E2 intrusion. The borehole from the previous intrusion is not represented explicitly in the model. Runs for the middle drilling location assume that the second or subsequent intrusion occurs at the location labeled in Figures 3-1 as the "middle well." Runs for the upper drilling location assume that the second or subsequent intrusion occurs at the location labeled "up-dip well" in Figure 3-1.

4.1.5 Scenario 5 (S5-DBR)

The BRAGFLO Salado flow modeling results from the S5-BF scenario are used as initial conditions to construct a second or subsequent intrusion into the repository in which a DBR may occur and in which the first intrusion occurs at 1,000 years without intersecting a Castile brine reservoir (Camphouse, 2012). Upper, middle, and lower second or subsequent intrusions are be modeled at 1,200, 1,400, 3,000, 5,000 and 10,000 years (3 locations × 5 intrusion times × 100 vectors = 1,500 calculations per replicate). The lower, middle, and upper drilling locations are treated the same as for the S4-DBR scenario.

4.2 Run Control

Run control, including code versions used and descriptions of code sequencing used to obtain DBR results in the PCS-2012 PA, are documented in Camphouse et al. (2012). PCS-2012 PA initial conditions and results obtained from BRAGFLO DBR pre- and post-processing, respectively, are contained in files with the names:

1. ALG2_DBR_AP161_Rr_Ss_Tttttt_Vvvv.CDB and
2. ALG3_DBR_AP161_Rr_Ss_Tttttt_ c_Vvvv.CDB,

where r (the replicate number) equals 1,2, or 3, s (the scenario number) equals 1,2,3,4,5, or 6, ttttt (time in years) equals 00550, 00750, 02000, 04000, or 10000, c (drilling location) is either L, M or U, and vvv (the vector number) is between 001 and 100. These files are located in CMS library LIBAP161_DBRRrSs under class AP161-0. PABC-2009 results used herein for purposes comparison have equivalent file names with 'AP161' replaced by 'PABC09', and are located in CMS library LIBPABC09_DBRRrSs under class PABC09-0.

Information Only

5 RESULTS

The DBR calculations over all three replicates of the PCS-2012 are presented in this section and compared to results from all three replicates of the PABC-2009. The analysis of the PABC-2009 results is described in Clayton (2008) and will only be summarized herein as appropriate. For consistency with previous analyses, non-zero volumes are defined as volumes that are greater than 10^{-7} m^3.

Each replicate of DBR calculations resulted in 7,800 (1,800 for first intrusion and 1,500×4= 6,000 for second intrusion) separate vector-scenario-drilling location-time combinations. These results are used as input to the code CCDFGF, which then calculates a release for any vector-intrusion time combination. This is done by first, linearly interpolating modeled volumes between the fixed intrusion times (Table 4-2) and second, multiplying the resulting intrusion-specific DBR volume with the radionuclide concentration calculated for that vector and intrusion time by the code PANEL (Garner 2010).

5.1 Summary

In this section, results from the PCS-2012 PA and the PABC-2009 are compared. Pertinent summary statistics for the calculations are listed in Table 5-1. The maximum DBR volumes shown in the table are over all three replicates, times, vectors and drilling locations. Overall there is a consistent increase in the maximum DBR volumes from PABC-2009 to PCS-2012 PA. The largest increases were observed in scenarios S4-DBR and S5-DBR which are associated with E2 intrusions. The BRAGFLO modeling results reported by Camphouse (2012b), show that E2 intrusion scenarios in the PCS-2012 PA yielded waste panel pressure that is higher, on average, than that seen in the PABC-2009 at the time of intrusion and it remains higher for the duration of the 10,000 year regulatory period. Similarly, the mean waste panel brine saturation is higher at the time of intrusion in the PCS-2012 PA, resulting in higher long-term waste panel brine saturations for E2 intrusion scenarios (Camphouse, 2012b). DBRs are strongly dependent on waste panel pressure and brine saturation at the time of intrusion. Hence, increases to these two quantities lead to the increased maximum DBR volumes observed in scenarios S4-DBR and S5-DBR, and to the higher overall number of non-zero brine volume vectors.

The moderate increases in maximum DBR volumes for scenarios S2-DBR and S3-DBR are due to the fact that the lower long-term permeability range of the ROMPCS as compared to Option D yields a period of increased waste panel pressurization following an E1 intrusion. The increased mean waste panel pressure slightly inhibits brine flow into the panel after the intrusion, resulting in only a slight decrease to the mean waste panel brine saturation as compared to PABC-2009 E1 intrusion results. The combination of increased pressure and a slight decrease to brine saturation yields an increase to the maximum DBR volume seen in the PCS-2012 PA E1 results.

For undisturbed conditions, implementation of the ROMPCS yields higher long-term waste panel pressure (on average) than was seen in the PABC-2009 (Camphouse, 2012b). The increase in mean waste panel pressure is accompanied by an increase in the average waste panel brine saturation for the ROMPCS results. The ROMPCS design allows more brine inflow to the waste panel during the first 200 years when compared to Option D results. This increased brine inflow,

Information Only

combined with the tightness of the ROMPCS after 200 years, results in increased waste panel gas generation (on average) and a subsequent increase to waste panel mean pressure. This explains the increase in the scenario S1-DBR maximum DBR volume for the PCS-2012 PA compared to the PABC-2009.

Table 5-1 shows a modest (~6%) increase in the number of non-zero DBR volumes for the PCS-2012 PA calculations compared with the PABC-2009, and modest increases in the average DBR volumes for all scenarios. These increases attributable to the increases in waste panel brine pressure and brine saturation discussed above and presented in more detail in Camphouse (2012b).

Table 5-1: Summary statistics for the PCS-2012 PA and PABC-2009 DBR calculations over all replicates and vectors.

	Number of Vectors		Maximum volume (m^3)		Average volume (m^3)	
Scenario	PABC-2009	PCS-2012 PA	PABC-2009	PCS-2012 PA	PABC-2009	PCS-2012 PA
S1-DBR	369	419	27.6	45.9	0.1	0.4
S2-DBR	1179	1174	48.2	52.9	2.8	2.9
S3-DBR	926	907	40.6	43.8	1.5	1.4
S4-DBR	211	281	20.4	42.5	0.1	0.2
S5-DBR	314	401	21.1	53.8	0.1	0.3
Overall	2999	3182	48.2	53.8	0.9	1.0

Note: The volume of direct brine released was obtained from the output variable BRIN_REL which is calculated in the ALGEBRACDB step 3 post-processing step, and contained in the ALG3 CDB files.

5.2 Direct Brine Releases from the Lower Drilling Location

Table 5-2 through Table 5-6 summarize the number of vectors for the PCS-2012 PA calculations with non-zero DBR volumes, and the maximum and average DBR volumes for the 300 vectors in each scenario-time-drilling location combination. The same summary statistics for the PABC-2009 are included in the tables for comparison.

One important result that is evident from Table 5-2 through Table 5-6 and has been reported consistently in previously analyses is that DBRs are less likely to occur in intrusions situated in the upper drilling location than in the lower drilling location. Of all the intrusions that had a non-zero DBR volume for the PCS-2012 PA, 63.4% occurred during a lower drilling intrusion, a modest decrease from the value of 66.5% for PABC-2009. Furthermore, of all the intrusions that had a non-zero DBR volume and occur during a lower drilling intrusion, 78.0% are found in scenarios S2-DBR and S3-DBR, a slight decrease from 82.9% for PABC-2009 (Clayton et al., 2010). Therefore, as has been observed previously (Clayton et al., 2010; Pasch and Camphouse, 2011), the majority of the non-zero DBR volumes occur when there is a previous E1 intrusion within the same panel. Not only are DBRs less likely to occur during upper drilling intrusions, but also the DBR volumes from such intrusions tend to be much smaller than those from lower drilling intrusions. For all three replicates of the PCS-2012 PA, the maximum DBR volume for the upper drilling location is 25.7 m^3 compared to 53.8 m^3 for the lower drilling location. These

Information Only

observations support the conclusion that lower drilling intrusions are the primary source for significant DBRs.

Figures 5-1 to 5-10 are probability plots of the DBR volumes for scenarios S1-DBR to S5-DBR for all three replicates. Results of the PCS-2012 PA are compared to those of the PABC-2009. The probability plots show the percentiles (x-axis) of the DBR volumes (y-axis). The plots of PCS-2012 PA results are generally similar to those of the PABC-2009. However, unlike the PABC-2009 where the largest DBR volume was observed in scenario S2-DBR, for the PCS-2012 PA the largest DBR volume occurs in scenario S5-DBR.

Information Only

Table 5-2: Summary table of number of vectors with non-zero, maximum and average DBR volumes over all three replicates for the S1-DBR calculations

Time (yrs)	Drilling Location	Number of Vectors		Maximum volume (m^3)		Average volume (m^3)	
		PABC-2009	PCS-2012 PA	PABC-2009	PCS-2012 PA	PABC-2009	PCS-2012 PA
100	L	0	0	0.00E+00	0.00E+00	0.00E+00	0.00E+00
350	L	0	0	0.00E+00	0.00E+00	0.00E+00	0.00E+00
1,000	L	26	40	1.51E+01	4.59E+01	1.80E-01	1.01E+00
3,000	L	37	52	5.92E+00	4.12E+01	1.16E-01	6.51E-01
5,000	L	46	55	2.19E+01	3.29E+01	2.92E-01	7.81E-01
10,000	L	46	56	2.03E+01	3.66E+01	4.26E-01	8.96E-01
100	M	0	0	0.00E+00	0.00E+00	0.00E+00	0.00E+00
350	M	0	0	0.00E+00	0.00E+00	0.00E+00	0.00E+00
1,000	M	19	23	6.33E+00	4.30E+01	5.14E-02	4.56E-01
3,000	M	32	33	2.27E+00	1.40E+01	3.95E-02	1.78E-01
5,000	M	29	32	2.25E+01	2.19E+01	1.24E-01	2.42E-01
10,000	M	31	30	2.76E+01	1.65E+01	1.32E-01	1.76E-01
100	U	0	0	0.00E+00	0.00E+00	0.00E+00	0.00E+00
350	U	0	0	0.00E+00	0.00E+00	0.00E+00	0.00E+00
1,000	U	16	17	6.15E+00	5.23E+00	4.75E-02	3.94E-02
3,000	U	29	27	1.73E+00	1.53E+00	3.13E-02	2.29E-02
5,000	U	28	26	2.02E+01	2.13E+01	7.82E-02	1.21E-01
10,000	U	30	28	1.91E+01	2.57E+01	9.37E-02	1.16E-01

Note: Volume releases less than 1×10^{-7} m^3 have been reduced to 0.0 for the purposes of this table. The maximum DBR volume is calculated as the maximum value of the 300 vectors for each replicate-scenario-time-drilling location combination. The average DBR volume is calculated by the total of the DBR volumes divided by the total number of vectors. The DBR volume was obtained from the output variable BRIN_REL which is calculated in the ALGEBRACDB step 3 post-processing step, and contained in the ALG3 CDB files.

Table 5-3: Summary table of number of vectors with non-zero, maximum and average DBR volumes over all three replicates for the S2-DBR calculations.

Time (yrs)	Drilling Location	Number of Vectors		Maximum volume (m^3)		Average volume (m^3)	
		PABC-2009	PCS-2012 PA	PABC-2009	PCS-2012 PA	PABC-2009	PCS-2012 PA
550	L	285	287	3.74E+01	4.01E+01	1.23E+01	1.19E+01
750	L	255	245	3.86E+01	3.80E+01	1.16E+01	1.10E+01
2,000	L	164	165	3.78E+01	4.43E+01	7.11E+00	7.93E+00
4,000	L	140	133	4.39E+01	4.43E+01	5.38E+00	5.82E+00
10,000	L	137	127	4.82E+01	5.29E+01	5.64E+00	5.10E+00
550	M	7	8	4.41E+00	1.33E+01	1.71E-02	5.40E-02
750	M	15	19	7.63E+00	2.98E+01	5.02E-02	3.45E-01
2,000	M	32	36	8.70E+00	3.38E+01	1.42E-01	3.27E-01
4,000	M	30	31	2.10E+01	1.04E+01	9.88E-02	1.39E-01
10,000	M	24	32	1.79E+01	1.37E+01	1.25E-01	1.77E-01
550	U	5	4	4.14E-01	4.38E-01	1.91E-03	1.67E-03
750	U	9	7	2.35E+00	1.16E-01	9.01E-03	6.33E-04
2,000	U	27	29	9.68E+00	7.25E+00	1.12E-01	9.15E-02
4,000	U	27	25	1.18E+00	8.23E-01	1.54E-02	1.02E-02
10,000	U	22	26	1.24E+01	2.46E+01	7.96E-02	1.14E-01

Note: Volume releases less than 1×10^{-7} m^3 have been reduced to 0.0 for the purposes of this table. The maximum DBR volume is calculated as the maximum value of the 300 vectors for each replicate-scenario-time-drilling location combination. The average DBR volume is calculated by the total of the DBR volumes divided by the total number of vectors. The DBR volume was obtained from the output variable BRIN_REL which is calculated in the ALGEBRACDB step 3 post-processing step, and contained in the ALG3 CDB files.

Table 5-4: Summary table of number of vectors with non-zero, maximum and average DBR volumes over all three replicates for the S3-DBR calculations.

Time (yrs)	Drilling Location	Number of Vectors		Maximum volume (m^3)		Average volume (m^3)	
		PABC-2009	PCS-2012 PA	PABC-2009	PCS-2012 PA	PABC-2009	PCS-2012 PA
1,200	L	231	221	3.68E+01	3.55E+01	8.76E+00	7.27E+00
1,400	L	166	159	3.25E+01	3.18E+01	5.41E+00	4.49E+00
3,000	L	96	85	2.68E+01	3.48E+01	2.47E+00	2.44E+00
5,000	L	90	74	3.76E+01	4.15E+01	2.70E+00	2.41E+00
10,000	L	90	77	4.06E+01	4.38E+01	2.76E+00	2.35E+00
1,200	M	27	32	1.81E+01	3.36E+01	1.58E-01	4.85E-01
1,400	M	32	35	1.98E+01	3.48E+01	2.13E-01	4.58E-01
3,000	M	29	34	3.59E+00	1.40E+01	4.48E-02	1.76E-01
5,000	M	26	30	2.17E+01	2.24E+01	1.21E-01	2.37E-01
10,000	M	21	32	1.34E+01	1.46E+01	6.40E-02	1.82E-01
1,200	U	23	22	4.39E+00	5.28E+00	4.45E-02	5.51E-02
1,400	U	23	24	2.64E+00	3.20E+00	3.60E-02	4.15E-02
3,000	U	29	31	1.95E+00	1.46E+00	3.39E-02	2.38E-02
5,000	U	24	25	1.96E+01	2.21E+01	7.33E-02	1.23E-01
10,000	U	19	26	1.22E+01	2.46E+01	7.35E-02	1.14E-01

Note: Volume releases less than 1×10^{-7} m^3 have been reduced to 0.0 for the purposes of this table. The maximum DBR volume is calculated as the maximum value of the 300 vectors for each replicate-scenario-time-drilling location combination. The average DBR volume is calculated by the total of the DBR volumes divided by the total number of vectors. The DBR volume was obtained from the output variable BRIN_REL which is calculated in the ALGEBRACDB step 3 post-processing step, and contained in the ALG3 CDB files.

Table 5-5: Summary table of number of vectors with non-zero, maximum and average DBR volumes over all three replicates for the S4-DBR calculations.

Time (yrs)	Drilling Location	Number of Vectors		Maximum volume (m^3)		Average volume (m^3)	
		PABC-2009	PCS-2012 PA	PABC-2009	PCS-2012 PA	PABC-2009	PCS-2012 PA
550	L	6	12	1.00E+00	3.17E+01	4.09E-03	2.33E-01
750	L	5	9	1.93E+01	1.62E+01	7.36E-02	2.19E-01
2,000	L	17	21	1.60E+01	4.25E+01	1.44E-01	6.19E-01
4,000	L	22	26	1.92E+01	3.52E+01	9.43E-02	4.04E-01
10,000	L	24	29	2.04E+01	3.91E+01	2.11E-01	6.97E-01
550	M	6	7	5.48E-01	1.17E+01	2.47E-03	4.94E-02
750	M	9	11	2.61E+00	2.57E+01	1.08E-02	1.82E-01
2,000	M	18	30	8.25E+00	3.30E+01	7.98E-02	3.25E-01
4,000	M	19	28	1.72E+00	1.02E+01	2.00E-02	1.29E-01
10,000	M	14	27	1.48E+00	1.49E+01	9.71E-03	1.75E-01
550	U	5	4	4.12E-01	4.35E-01	1.89E-03	1.63E-03
750	U	8	6	2.05E+00	1.12E-01	7.93E-03	6.00E-04
2,000	U	22	25	9.60E+00	6.89E+00	1.05E-01	8.01E-02
4,000	U	21	24	1.21E+00	9.62E-01	1.26E-02	1.14E-02
10,000	U	15	22	1.11E+01	2.44E+01	5.08E-02	1.15E-01

Note: Volume releases less than 1×10^{-7} m^3 have been reduced to 0.0 for the purposes of this table. The maximum DBR volume is calculated as the maximum value of the 300 vectors for each replicate-scenario-time-drilling location combination. The average DBR volume is calculated by the total of the DBR volumes divided by the total number of vectors. The DBR volume was obtained from the output variable BRIN_REL which is calculated in the ALGEBRACDB step 3 post-processing step, and contained in the ALG3 CDB files.

Table 5-6: Summary table of number of vectors with non-zero, maximum and average DBR volumes over all three replicates for the S5-DBR calculations.

Time (yrs)	Drilling Location	Number of Vectors		Maximum volume (m^3)		Average volume (m^3)	
		PABC-2009	PCS-2012 PA	PABC-2009	PCS-2012 PA	PABC-2009	PCS-2012 PA
1,200	L	31	50	1.97E+01	4.21E+01	3.17E-01	1.14E+00
1,400	L	15	18	2.11E+01	4.12E+01	2.05E-01	5.66E-01
3,000	L	18	21	6.01E+00	4.04E+01	6.79E-02	3.87E-01
5,000	L	23	25	9.25E+00	3.43E+01	6.25E-02	4.34E-01
10,000	L	24	29	2.03E+01	5.38E+01	2.10E-01	7.45E-01
1,200	M	25	29	1.81E+01	3.42E+01	1.53E-01	4.24E-01
1,400	M	26	33	1.98E+01	3.53E+01	2.11E-01	4.65E-01
3,000	M	21	31	4.17E+00	1.41E+01	4.01E-02	1.72E-01
5,000	M	19	26	1.58E+00	1.05E+01	1.28E-02	1.55E-01
10,000	M	14	27	1.48E+00	1.42E+01	1.02E-02	1.74E-01
1,200	U	21	20	4.32E+00	4.15E+00	3.56E-02	3.74E-02
1,400	U	20	22	2.67E+00	3.59E+00	3.81E-02	4.21E-02
3,000	U	23	25	2.03E+00	1.54E+00	3.13E-02	2.42E-02
5,000	U	19	23	1.15E+00	1.19E+01	7.91E-03	4.73E-02
10,000	U	15	22	1.11E+01	2.44E+01	5.03E-02	1.15E-01

Note: Volume releases less than 1×10^{-7} m^3 have been reduced to 0.0 for the purposes of this table. The maximum DBR volume is calculated as the maximum value of the 300 vectors for each replicate-scenario-time-drilling location combination. The average DBR volume is calculated by the total of the DBR volumes divided by the total number of vectors. The DBR volume was obtained from the output variable BRIN_REL which is calculated in the ALGEBRACDB step 3 post-processing step, and contained in the ALG3 CDB files.

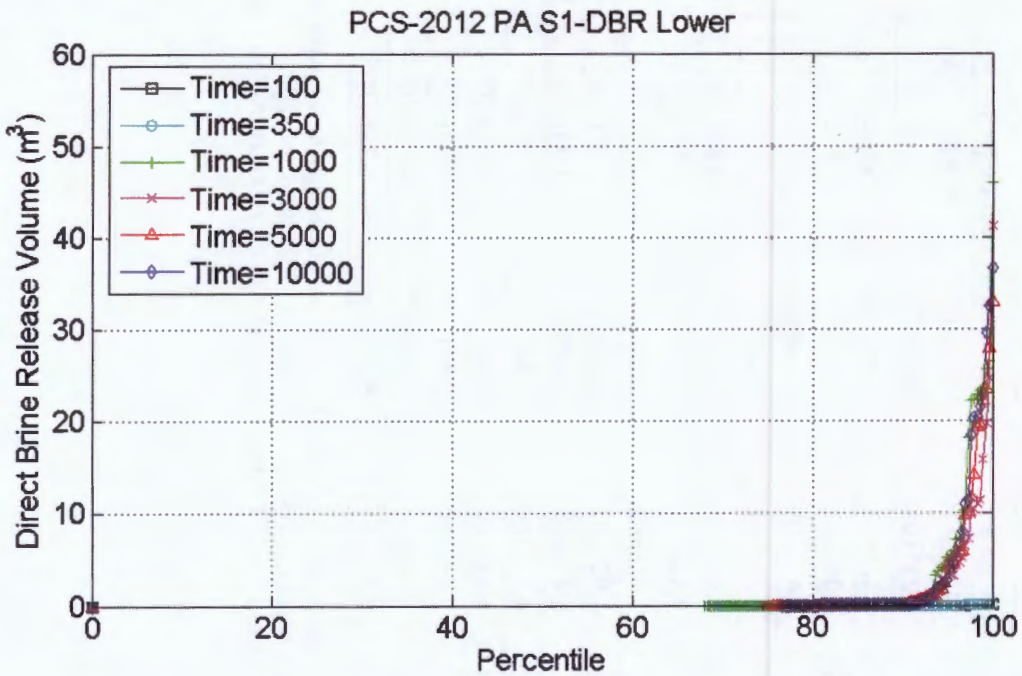

Figure 5-1: PCS-2012 PA lower intrusion DBR volume percentile rankings for all replicates and vectors of the scenario S1-DBR.

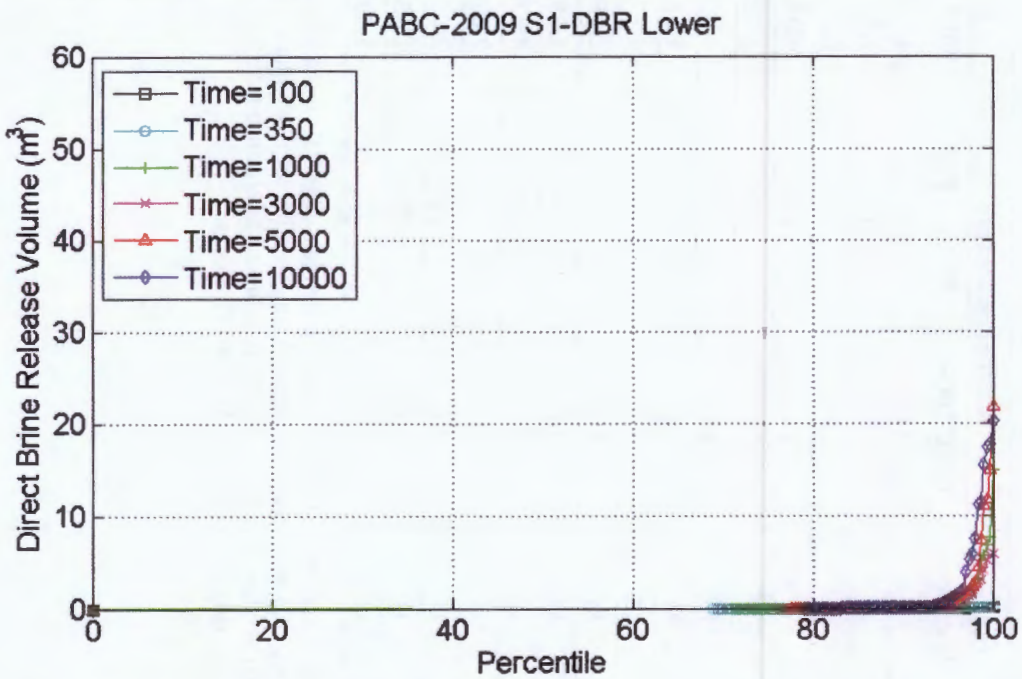

Figure 5-2: PABC-2009 lower intrusion DBR volume percentile rankings for all replicates and vectors of scenario S1-DBR.

Information Only

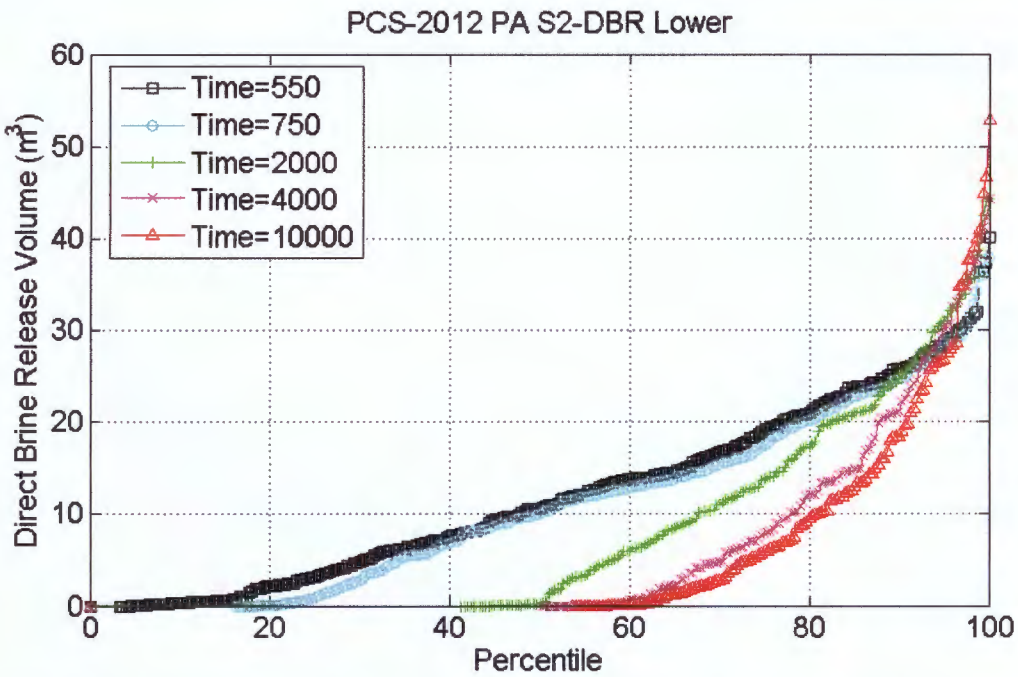

Figure 5-3: PCS-2012 PA lower intrusion DBR volume percentile rankings for all replicates and vectors of scenario S2-DBR.

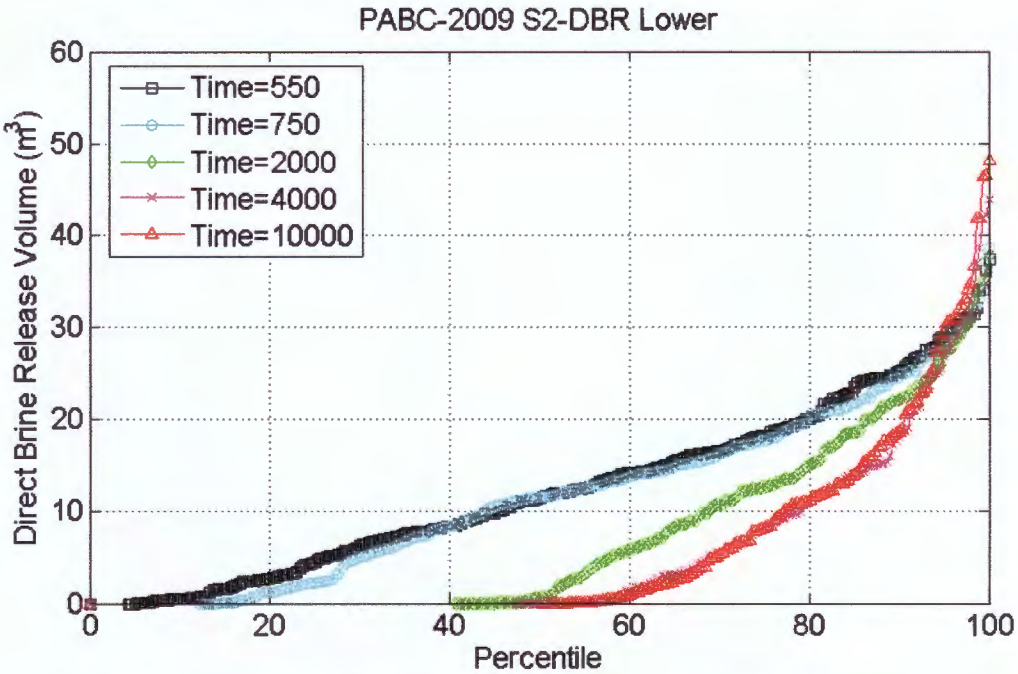

Figure 5-4: PABC-2009 lower intrusion DBR volume percentile rankings for all replicates and vectors of scenario S2-DBR.

Information Only

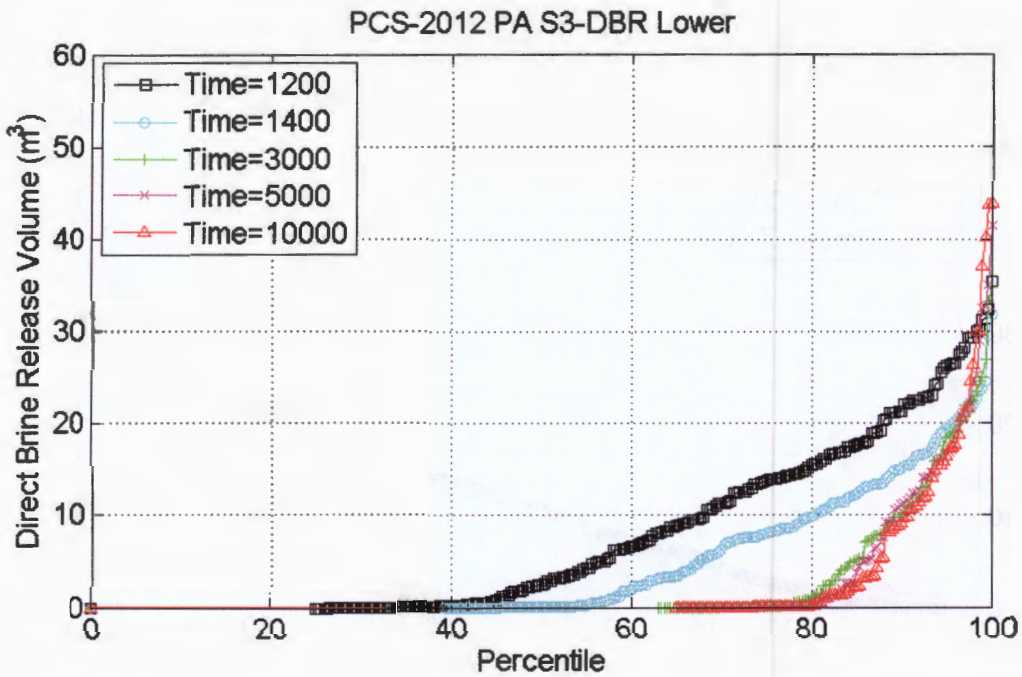

Figure 5-5: PCS-2012 PA lower intrusion DBR volume percentile rankings for all replicates and vectors of scenario S3-DBR.

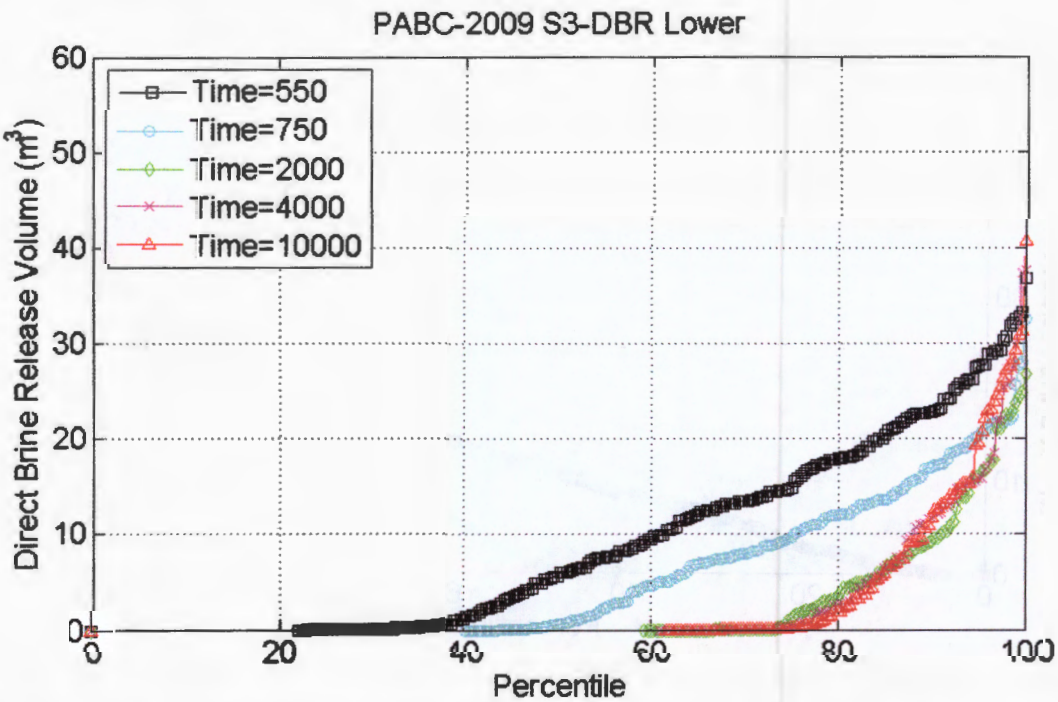

Figure 5-6: PABC-2009 lower intrusion DBR volume percentile rankings for all replicates and vectors of scenario S3-DBR.

Information Only

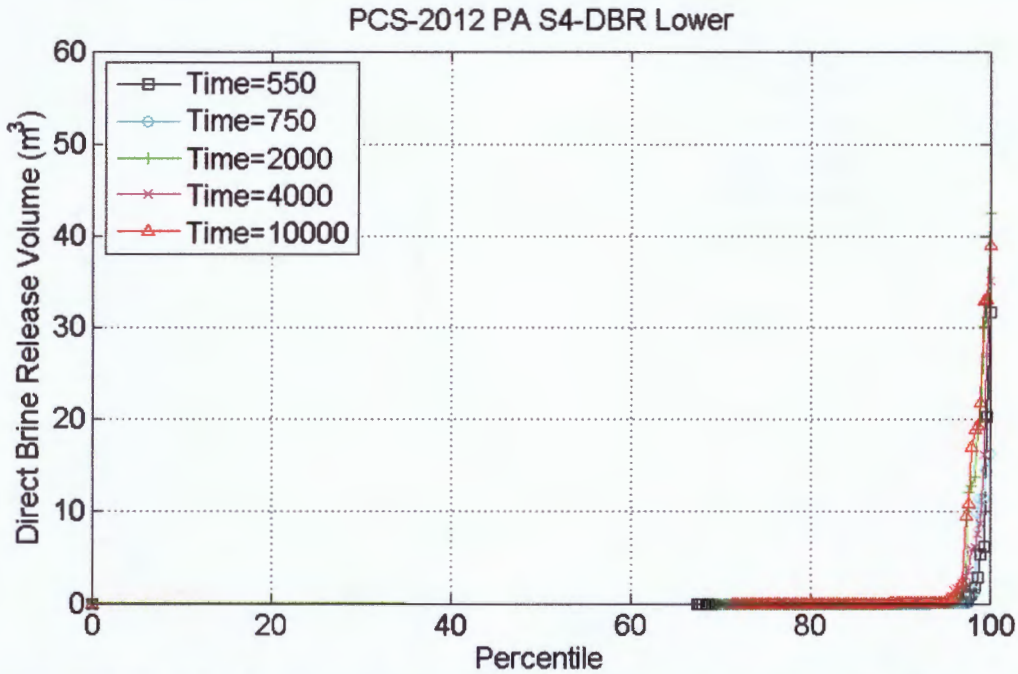

Figure 5-7: PCS-2012 PA lower intrusion DBR volume percentile rankings for all replicates and vectors of scenario S4-DBR.

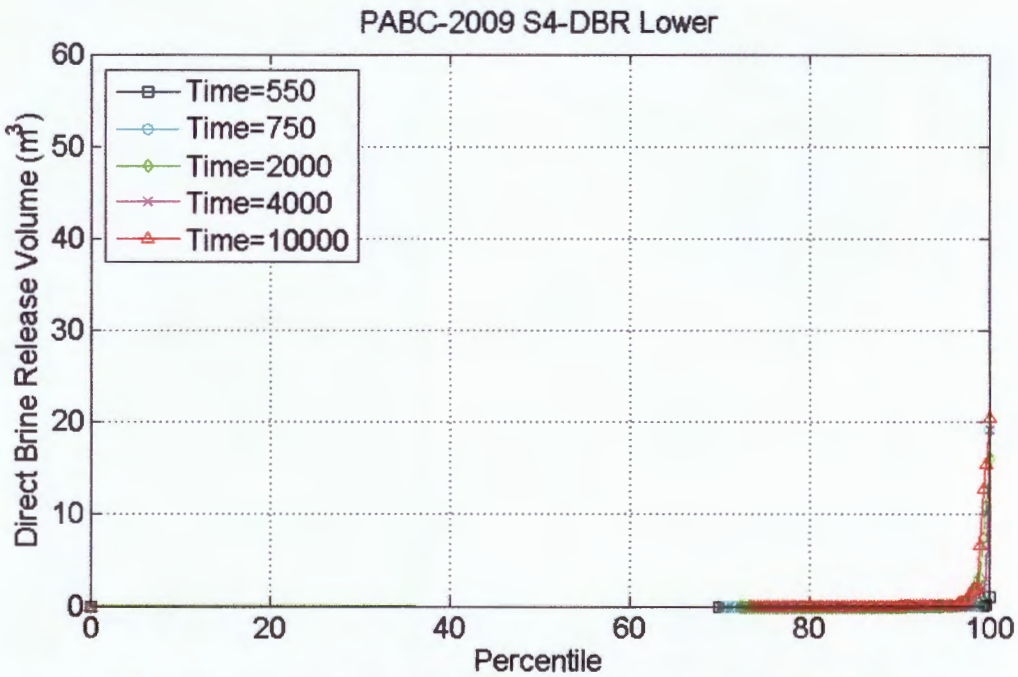

Figure 5-8: PABC-2009 lower intrusion DBR volume percentile rankings for all replicates and vectors of scenario S4-DBR.

Information Only

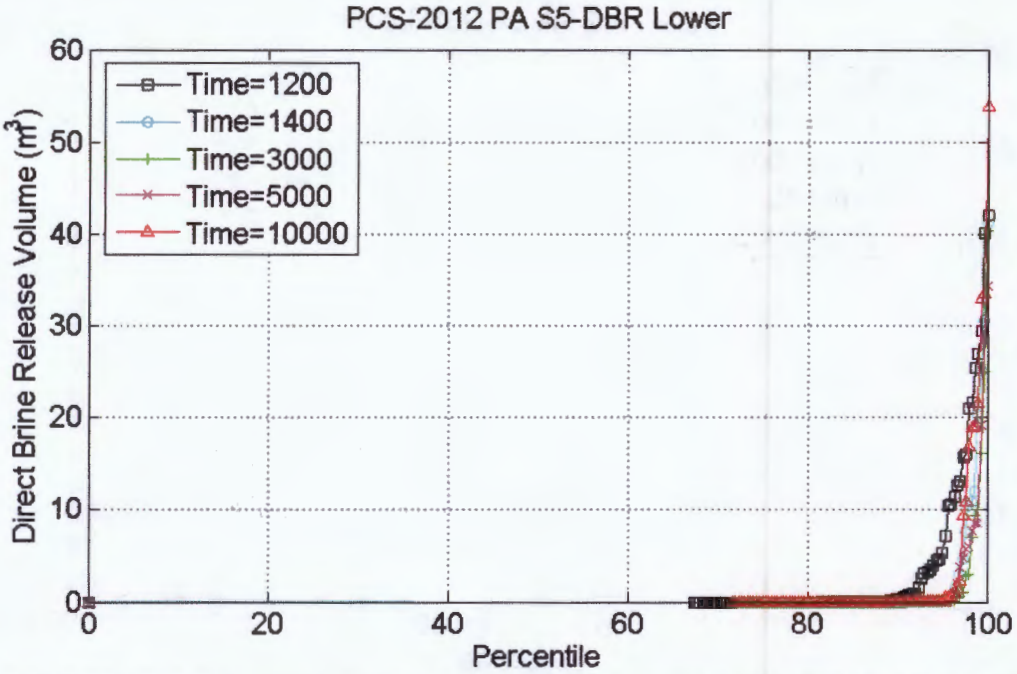

Figure 5-9: PCS-2012 PA lower intrusion DBR volume percentile rankings for all replicates and vectors of scenario S5-DBR.

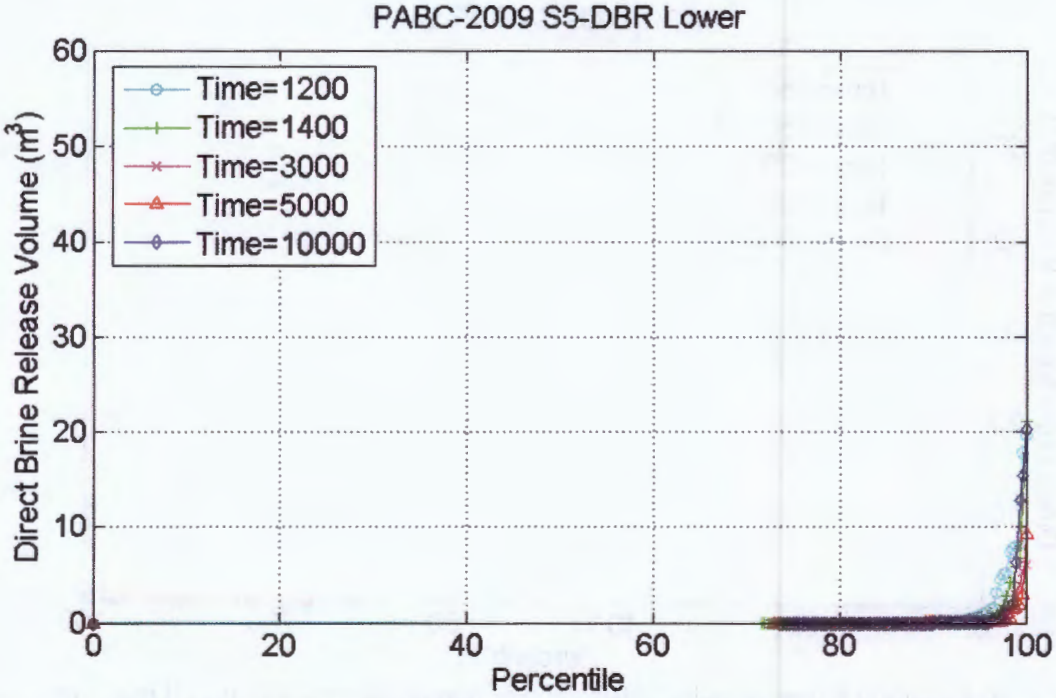

Figure 5-10: PABC-2009 lower intrusion DBR volume percentile rankings for all replicates and vectors of scenario S5-DBR.

Information Only

5.3 Sensitivity of Direct Brine Releases to Input Parameters

Volume averaged brine pressure and brine saturation in the intruded panel are the two most important variables that control DBR volumes (Clayton 2008). The sensitivity of the DBR volumes to these two variables is discussed qualitatively here. For the plots given below, the values of these parameters were extracted from the ALG2 files from the DBR calculations.

Scenarios S2-DBR and S3-DBR have significant DBR volumes because the presence of a previous borehole connecting the repository to the Castile brine reservoir has the general effect of simultaneously increasing the waste panel pressure and brine saturation. The sensitivity analysis presented here focuses on scenarios S2-DBR and S3-DBR because these scenarios have the greatest number of significant DBR volumes. As in previous DBR analyses performed hitherto, scenarios S1-DBR, S4-DBR, and S5-DBR have very few runs with non-zero DBR volumes and are thus excluded from the sensitivity analysis presented herein. Due to the close similarity between scenarios S2-DBR and S3-DBR, only scenario S2-DBR is discussed in the sensitivity analysis.

Volume averaged brine pressure in the intruded panel at the time of the intrusion is an important factor for many vectors. Figure 5-11 and Figure 5-12 show scenario S2-DBR scatter plots of DBR volume versus pressure in the intruded panel at different intrusion times for the case of a lower (down-dip) location of drilling intrusion for the PCS-2012 PA and the PABC-2009, respectively. As prescribed by the conceptual model, there are no DBRs until the brine pressure exceeds the hydrostatic threshold of 8 MPa, indicated in the figures by the vertical line. Above 8 MPa, there is still a significant number of vectors having zero DBR volumes; these vectors have associated mobile brine saturations that are less than zero and thus no brine is available in a mobile form to be released (Clayton et al., 2010). Figure 5-13 and Figure 5-14 show scatter plots of the same data as in Figures 5-11 and 5-12 but for different mobile brine saturation ranges. They show that DBR volumes tend to increase with increasing pressure and increasing mobile brine saturation, the variables to which DBR volumes are historically sensitive.

As the case was with the PABC-2009 results reported in Clayton et al. (2010) and reproduced here in Figures 5-12 and 5-14, the PCS-2012 PA results in Figures 5-11 and 5-13 show a clustering of the data about a linear trend (dashed line in the figures) with a slope of about 8 m^3/MPa and intersecting the pressure axis at 8 MPa. Comparing results in Figure 5-11 to those in Figure 5-13 reveals that the linearity of the clustering is more strongly dependent on mobile brine saturation than it is on intrusion time. The results further indicate that the linearity of the correlation between pressure and DBR volumes increases with increasing mobile brine saturation.

Figure 5-15 and Figure 5-16 are plots of mobile brine saturation versus pressure for the S2-DBR scenario for all intrusion times with symbols indicating the range of DBR volumes, for the PCS-2012 PA and the PABC-2009, respectively. Though these figures do not show any meaningful correlation between mobile brine saturation and brine pressure, they show the general increase in DBR volume with both brine saturation and pressure alluded to above, with only modest differences between the PCS-2012 PA and PABC-2009 results.

Information Only

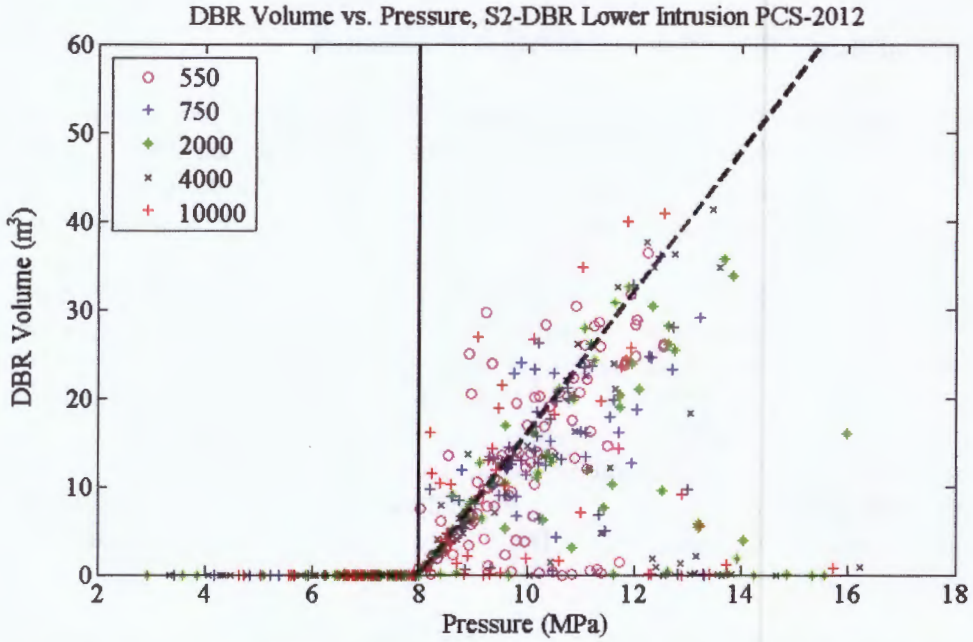

Figure 5-11: Scatter plot of DBR volume versus pressure in the intruded panel for replicate 1, S2-DBR scenario, lower drilling intrusion, PCS-2012 PA. Symbols indicate intrusion times in years.

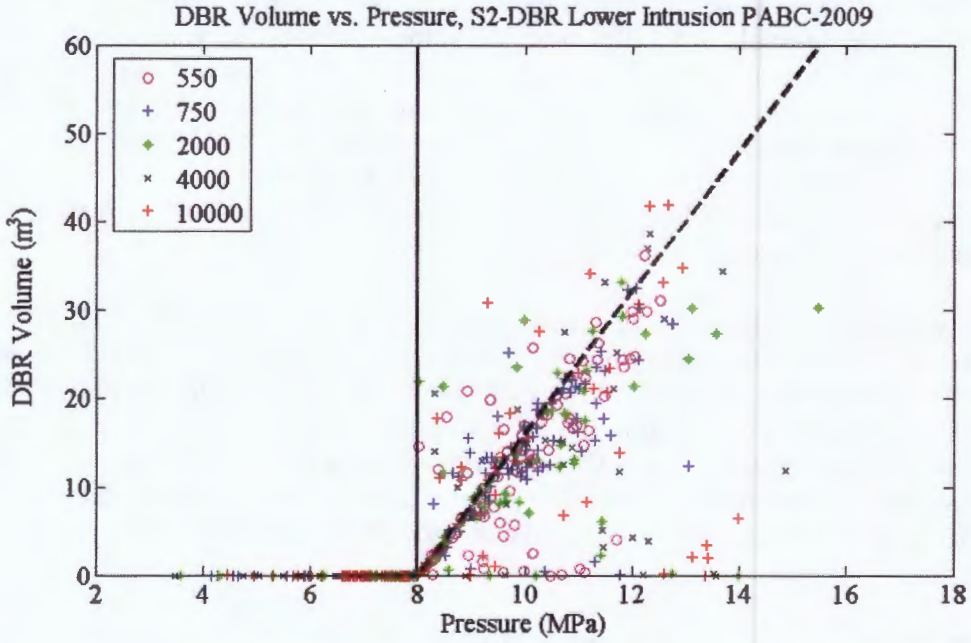

Figure 5-12: Scatter plot of DBR volume versus pressure in the intruded panel for replicate 1, S2-DBR scenario, lower drilling intrusion, PABC-2009. Symbols indicate intrusion times in years.

Information Only

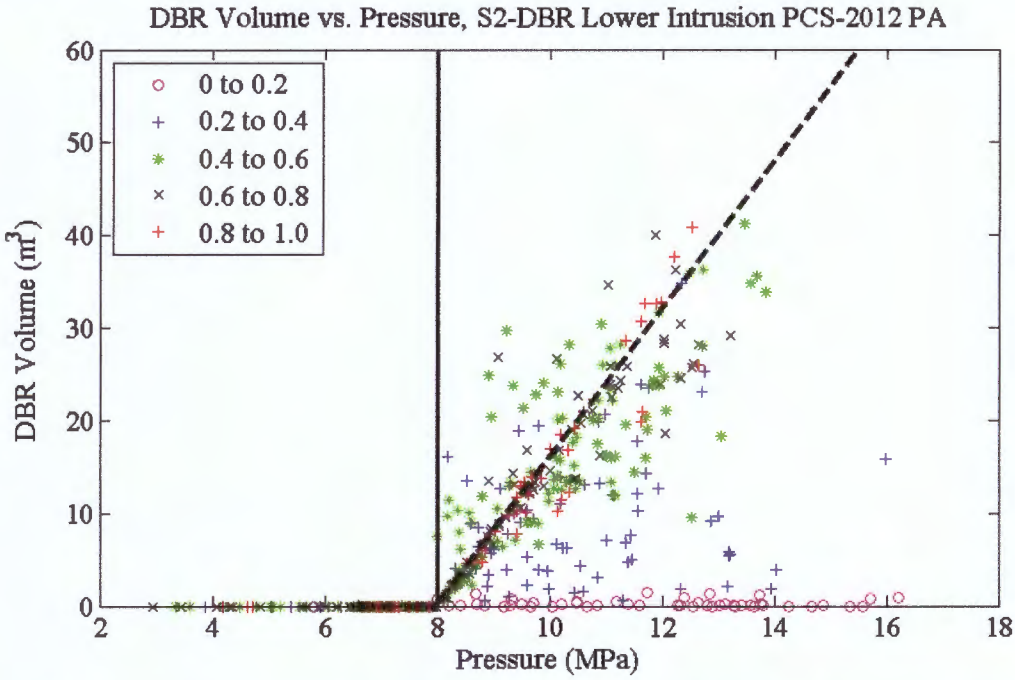

Figure 5-13: Scatter plot of DBR volume versus pressure in the intruded panel for replicate 1, S2-DBR scenario, lower drilling intrusion, PCS-2012 PA. Symbols indicate the range of mobile brine saturation (dimensionless).

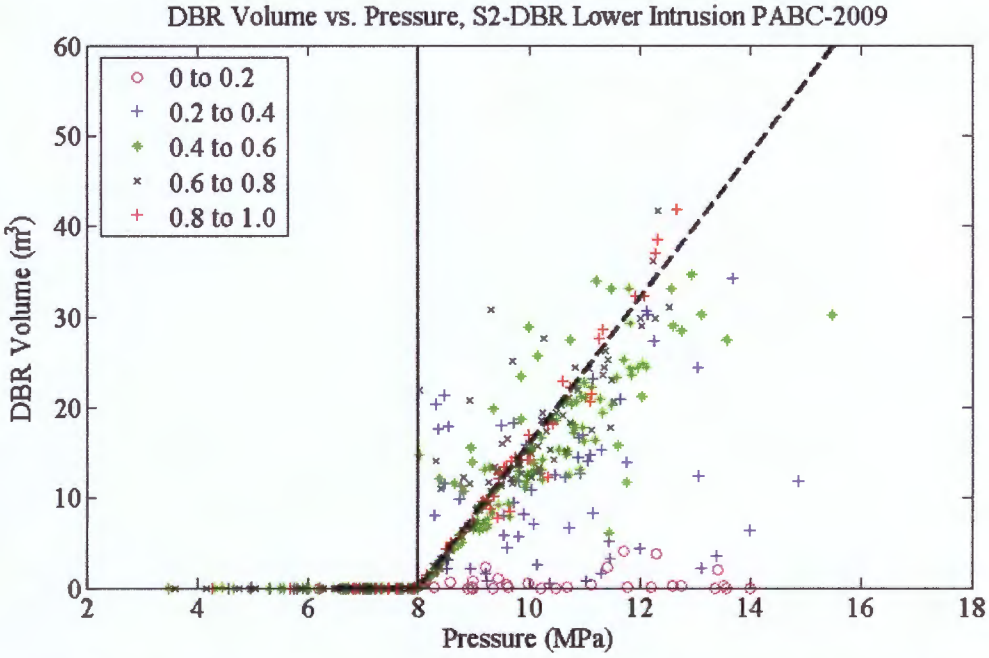

Figure 5-14: Scatter plot of DBR volume versus pressure in the intruded panel for replicate 1, S2-DBR scenario, lower drilling intrusion, PABC-2009. Symbols indicate the range of mobile brine saturation (dimensionless).

Information Only

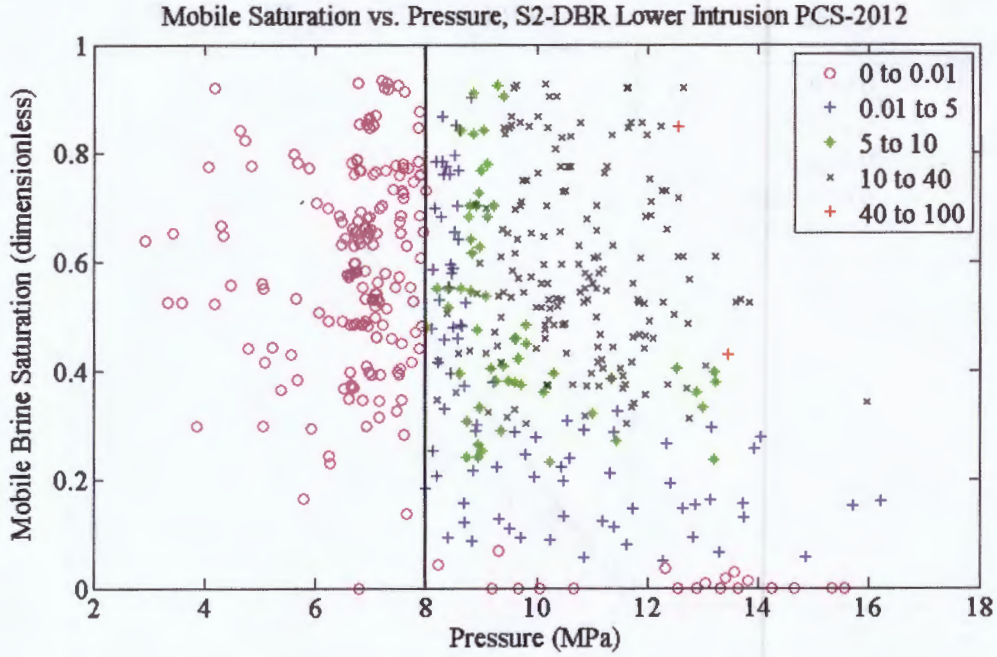

Figure 5-15: Scatter plot of mobile brine saturation versus pressure for replicate 1, S2-DBR scenario, lower drilling intrusion, all intrusion times, PCS-2012 PA. Symbols indicate the range of DBR volumes in m^3.

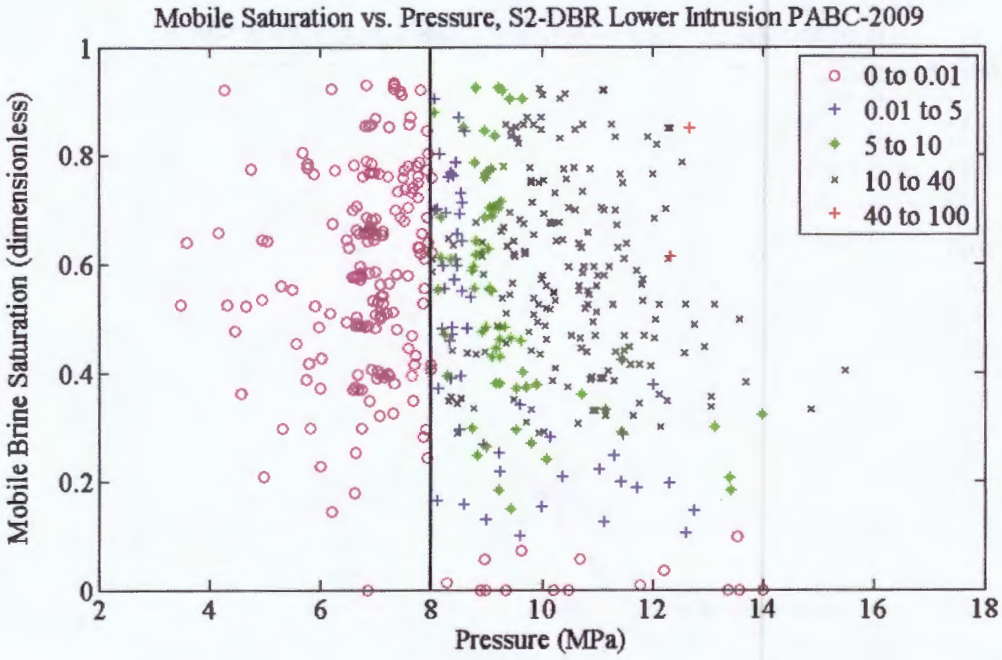

Figure 5-16: Scatter plot of mobile brine saturation versus pressure for replicate 1, S2-DBR scenario, lower drilling intrusion, all intrusion times, PABC-2009. Symbols indicate the range of DBR volumes in m^3.

Information Only

6 CONCLUSIONS

The DBR results from all three replicates of the PCS-2012 PA and PABC-2009 show that direct brine releases to the surface are very unlikely for most intrusions into the repository and in most cases such intrusions result in non-zero but inconsequential DBR volumes. The exception to this statement is for intrusions into a panel that had previously been intruded by an earlier bore hole that had also intruded an underlying pressurized Castile brine reservoir. Such intrusions are represented in PA by the lower drilling intrusions in the scenarios S2-DBR and S3-DBR. Based on a comparison of the results from the PCS-2012 PA to those from the PABC-2009, it is concluded that the PCS-2012 PA maximum DBR volumes are higher for each scenario, the frequency of DBR releases is slightly (almost imperceptibly) higher, and the variability in DBR volumes is higher. As in previous analyses, these results have been explained in terms of the parameters that affect DBR volumes.

7 REFERENCES

Camphouse, R.C. 2012a. Analysis Plan for the 2012 WIPP Panel Closure System Performance Assessment. AP-161, Revision 0. Sandia National Laboratories, Carlsbad, NM. ERMS 557726.

Camphouse, R.C. 2012b. Analysis Package for Salado Flow Modeling Done in the AP-161 (PCS-2012) Performance Assessment. Sandia National Laboratories, Carlsbad, NM. ERMS 558204.

Camphouse, R.C., D.C. Kicker, T.B. Kirchner, J.J. Long, B. Malama, and Zeitler, T.R. 2012. Summary Report and Run Control for the 2012 WIPP Panel Closure System Performance Assessment. Sandia National Laboratories, Carlsbad, NM. (in preparation)

Chappelear, J.E. and A.S. Williamson. 1981. Representing Wells in Numerical Reservoir Simulation. ERMS 249488.

Clayton, D.J. 2008. Analysis Package for Direct Brine Releases: Compliance Recertification Application – 2009. Sandia National Laboratories, Carlsbad, NM. ERMS 548571.

Clayton, D.J. 2010. Analysis Package for Direct Brine Releases: CRA-2009 Performance Assessment Baseline Calculation, Revision 0. Sandia National Laboratories. Carlsbad, NM. ERMS 552829.

Clayton, D.J., R.C. Camphouse, J.W. Garner, A.E. Ismail, T.B. Kirchner, K.L. Kuhlman, and M.B. Nemer. 2010. Summary Report of the CRA-2009 Performance Assessment Baseline Calculation. Sandia National Laboratories, Carlsbad, NM. ERMS 553039.

Hansen, C. W. 2002. Analysis Report for the Panel Closure Impact Assessment. Sandia National Laboratories, Carlsbad, NM. ERMS 523935.

Helton, J.C, J.E. Bean, F.W. Berglund, F.J. Davis, K. Economy, J.W. Garner, J.D. Johnson, R.J. MacKinnon, J. Miller, D.G. O'Brien, J.L. Ramsey, J.D. Schreiber, A. Shinta, L.N. Smith, D.M. Stoelzel, C. Stockman and P. Vaughn. 1998. Uncertainty and Sensitivity Analysis Results Obtained in the 1996 Performance Assessment for the Waste Isolation Pilot Plant. Sandia National Laboratories, Albuquerque, NM. SAND98-0365, ERMS 252619.

Information Only

Kirkes, G.R. 2011. Features, Events and Processes Assessment for Changes Described in Analysis Plan – 151, Revision 0. Sandia National Laboratories, Carlsbad, NM. ERMS 555237

Lee, J. 1982. Well Testing. SPE Textbook Series Vol. 1. New York, NY: Society of Petroleum Engineers of AIME.

Mattax, C.C. and R.L. Dalton. 1990. Reservoir Simulation. Henery L. Doherty Memorial Fund Society of Petroleum Engineers Inc., Richardson, TX.

Nemer, M.B. 2010. Analysis Package for Salado Flow Modeling: CRA-2009 Performance Assessment Baseline Calculation. Sandia National Laboratories. Carlsbad, NM. ERMS 552956

Pasch, J. and C. Camphouse, 2011. Analysis Package for Direct Brine Releases: Panel Closure Redesign and Repository Reconfiguration Performance Assessment (PC3R PA), Revision 0. Sandia National Laboratories. Carlsbad, NM. ERMS 555249.

Stoelzel, D.M. and D.G. O'Brien. 1996. Conceptual Model Description of BRAGFLO Direct Brine Release Calculations to Support the Compliance Certification Application (CCA MASS Attachment 16-2). U.S. Department of Energy, Carlsbad, NM. ERMS 239090.

U.S. Environmental Protection Agency (EPA). 1998. 40 CFR 194, Criteria for the Certification and Recertification of the Waste Isolation Pilot Plant's Compliance with the Disposal Regulations: Certification Decision: Final Rule. Federal Register, Vol. 63, 27354-27406. ERMS 251924.

U.S. Environmental Protection Agency (EPA). 2010. 40 CFR Part 194 Criteria for the Certification and Recertification of the Waste Isolation Pilot Plant's Compliance With the Disposal Regulations: Recertification Decision, Federal Register No. 222, Vol. 75, pp. 70584-70595, November 18, 2010.

Vugrin, E.D. and S.C. Dunagan. 2006. Analysis Package for the Impact Assessment of the Redesigned WIPP Panel Closure. Sandia National Laboratories, Carlsbad, NM. ERMS 543865.

Information Only